Analyst

Cite this: *Analyst*, 2012, **137**, 3314

www.rsc.org/analyst

PAPER

Ultrasensitive electrochemiluminescence detection of DNA based on nanoporous gold electrode and PdCu@carbon nanocrystal composites as labels†

Mei Yan,[a] Meng Zhang,[a] Shenguang Ge,[b] Jinghua Yu,*[a] Meng Li,[a] Jiadong Huang[a] and Su Liu[a]

Received 25th February 2012, Accepted 10th May 2012
DOI: 10.1039/c2an35267b

A sensitive electrochemiluminescence (ECL) DNA biosensor based on nanoporous gold (NPG) electrode and PdCu@carbon nanocrystals (CNCs) composites is developed. The CNCs were obtained simply by electrooxidation with abundant carboxyl groups at their surfaces. The NPG can be easily prepared by a selective dissolution of silver from silver–gold alloy in nitric acid, which has free-standing noble metal membranes with controllable three-dimensional (3D) porosity. The PdCu bimetallic nanocomposites with hierarchically hollow structures were fabricated through a simple replacement reaction using dealloyed nanoporous copper (NPC) as both a template and reducing agent. Structure characterization was obtained by means of transmission electron microscope (TEM) and scanning electron microscope (SEM) images. The PdCu@CNCs composites exhibit 6 times higher ECL intensity than the pure CNC-labeled reporter DNA. Taking advantage of dual-amplification effects of the developed probe, a limit of detection as low as 18 aM can be achieved and the assay exhibits excellent selectivity for single-mismatched DNA detection even in human serum. The proposed ECL based method should have wide applications in diagnosis of genetic diseases due to its simplicity, low cost, and high sensitivity at extremely low concentrations.

1. Introduction

DNA hybridization detection has recently attracted much attention due to its diverse applications including clinical diagnosis, environmental monitoring, and the detection and characterization of viruses, bacteria, and parasites.[1–3] It is essential to develop precise and convenient DNA sensors at extremely low concentration. Traditional methods for detection of DNA hybridization, such as membrane blots or gel electrophoresis, are slow and labor-intensive. Various DNA biosensors have been established including optical,[4–6] quartz-crystal microbalance,[7,8] electrochemical,[9,10] electrochemiluminescence (ECL),[11] and surface plasmon resonance techniques.[12] In these DNA biosensors, ECL biosensors are very promising due to its simplicity, low cost, high sensitivity and ease of control.[13,14] Sensitive detection of specific nucleic acid sequences on the basis of the hybridization reaction can be improved by target or signal amplification strategies.

Luminescent nanostructures have generated much excitement for a wide variety of promising applications, especially in optoelectronic devices,[15] biological labeling,[16] and biomedicine.[17] Semiconductor quantum dots (QDs) such as CdSe and the related core–shell nanocrystals are usually used. However, the release of a Cd^{2+} ion can result in a cytotoxic effect and is a potential environmental hazard, which limits the application of QDs.[18] Therefore, it is urgent to search for environment-friendly fluorescent nanoparticles. Compared with conventional organic dyes and semiconductor QDs, photoluminescent carbon nanocrystals (CNCs) are superior in terms of chemical inertness, large two-photon excitation cross-sections, lack of blinking, low cytotoxicity, and excellent biocompatibility.[19–22] Among these fluorescent carbon-based nanomaterials including nanotubes,[23–25] fullerenes,[26] and nanoparticles,[27–30] CNCs are highly promising due to their relatively high quantum yield and small size. Herein, fluorescent CNCs were prepared easily and simply by electrooxidation of graphite in aqueous solution with low cytotoxicity and no photobleaching, followed by a convenient separation. The as-prepared CNCs had abundant carboxyl groups at their surfaces, and exhibited strong ECL activity.

Recently, nanoporous metals obtained by dealloying have aroused great interest with their high surface area, low density, and three-dimensional (3D) bicontinuous pore–ligament structure.[31] Notably, nanoporous copper (NPC, obtained by dealloying CuAl alloy) has been demonstrated to be a good +3D

[a]*Key Laboratory of Chemical Sensing & Analysis in Universities of Shandong(University of Jinan), Chemistry and Chemical Engineering, University of Jinan, Jinan 250022, China. E-mail: ujn.yujh@gmail.com; Fax: +86-531-82765969*
[b]*Shandong Provincial Key Laboratory of Fluorine Chemistry and Chemical Materials, School of Chemistry and Chemical Engineering, University of Jinan, Jinan 250022, China*

† Electronic supplementary information (ESI) available. See DOI: 10.1039/c2an35267b

skeleton of nanoporosity, which is environmentally benign and is an effective fabrication route to hollow nanostructures with desired properties.[32] By a simple replacement reaction between NPC and noble metal salts (K_2PdCl_4), novel Pd-based nanotubular mesoporous bimetallic materials were successfully prepared with uniform structural dimensions, controllable composition, and interesting structure-dependent electrocatalytic properties. The nanoporous metallic structures are promising in electrocatalysis,[33,34] sensing,[35] and optics[36] due to the ease of mass transport and high electron conductivity they can afford. Herein, we have successfully fabricated nanotubular mesoporous PdCu bimetallic with hierarchically hollow nanostructures that shows novel nanotubular mesoporous morphology and high activity with a nanoporous shell. The PdCu alloys linked with CNCs (PdCu@CNCs composites) can be used as excellent ECL labels.

In the present work, we describe the development of a new version of the ECL biobarcode assay, in which PdCu bimetallic nanostructures instead of double labeling oligonucleotides is used as a new kind of biobarcode. It is well-known that cysteamine is a kind of sulfur containing biomolecule. In this system, the sulfur atoms of the cysteamine are applied to bind to the PdCu surface while the amino groups are employed for the attachment of CNCs. We have demonstrated that the utilization of cost-effective cysteamine conjugated PdCu alloys with CNCs can overcome disadvantages of conventional ECL signal probe, simplifying analytical procedure and shortening analysis time. Recently, the nanoporous gold (NPG) has attracted considerable attention in recent years due to its high surface-to-volume reaction, high in-plane conductivity, good stability and biocompatibility. NPG can be easily prepared by a selective dissolution of silver from silver–gold alloy in nitric acid, which has free-standing noble metal membranes with controllable 3D porosity.[31] This novel ECL assay based on NPG modified electrode and PdCu@CNCs composites biobarcode amplification can quantitatively detect DNA with high speed and sensitivity, and the detection limit of the current work is as low as 18 aM. Furthermore, it demonstrates excellent specificity for single-base mismatched and perfectly matched oligonucleotides even in human serum. We expect these PdCu@CNCs composites to perform as excellent ECL labels as well as the NPG electrode based ECL technology to open new perspectives in the development of tools for analytical chemistry.

2. Experimental

2.1. Reagents

All oligonucleotides were synthesized and purified from Shanghai Linc-Bio Science Co. LTD (Shanghai, China). The 100 nm thick white gold foils (Au–Ag alloy, 50 : 50 wt%) were obtained from Monarch. 6-Mercapto-1-hexanol (MCH) was purchased from Nanoport. Co. Ltd. (Shenzhen, China). Tris-(2-carboxyethyl)phosphine hydrochloride (TCEP), *N*-(3-dimethylaminopropyl)-*N*′-ethylcarbodiimide (EDC) and *N*-hydroxysuccinimide (NHS, 98%) were obtained from Alfa Aesar China Ltd. Chloroauric acid ($HAuCl_4 \cdot 4H_2O$) was purchased from Shanghai Chemical Reagent Company (Shanghai, China). All chemicals and solvents used were analytical grade or the highest purity available and were used as received. The sequences of oligonucleotides are presented with the following sequences:

Capture DNA (S_1)-5′-SH–$(CH_2)_6$–TCGTACGATCGATCC-3′; target DNA (S_2)-5′-GCCGCTCACACGATATTTTTTT TGGATCGATCGTACGA-3′; reporter DNA (S_3)-5′-TATCG TGTGAGCGGCTTTTTTTT–$(CH_2)_6$–SH-3′; single-mismatched DNA(S_4)-5′-GCCGCTCACACGATATTTTTTTT GGATCGATGGTACGA-3′; noncomplementary DNA (non-*c*DNA) (S_5)-5′-ACATGCTTGGACTGCTTTTTTTTCAGG CTCATCGTACG-3′.

All solutions were prepared using Milli-Q water (Millipore) as a solvent. The buffers involved in this work are as follows: DNA immobilization buffer, 10 mM Tris-HCl, 1.0 mM EDTA, 1.0 M NaCl, and 1.0 mM TCEP (pH 7.4); DNA hybridization buffer, 10 mM Tris-HCl, 1.0 mM EDTA, and 1.0 M NaCl (pH 7.4). Buffer for ECL, 10 mM Tris-HCl buffer (pH 7.4) containing 0.1 M $K_2S_2O_8$ and 0.1 M KCl as the coreactant.

2.2. Apparatus

The ECL measurements were carried out on a flow injection luminescence analyzer (IFFM-E, Xi'an Remex Electronic Instrument High-Tech Ltd., Xi'an, China) with the voltage of the photomultiplier tube (PMT) set at 800 V. Cyclic voltammetric measurements (CVs) were performed with a CHI 760D electrochemical workstation (Shanghai CH Instruments, China). Transmission electron microscopy (TEM) images were obtained from a Hitachi H-800 microscope (Japan). High resolution transmission electron microscopy (HRTEM) images of the prepared CNCs were recorded on an electronic microscope (Tecnai G2 F20S-TWIN 200 KV). The morphologies of NPC were characterized with a scanning electronic microscope (SEM) on a HITACHI S-3500 SEM. Integrated photoluminescence (PL) measurements were performed at room temperature using a LS–55 spectrofluorometer (P.E. USA). UV-vis absorption spectra were recorded with a UV–3101 spectrophotometer (SHIMADZU, Japan). All experiments were carried out with a conventional three-electrode system with the modified glassy carbon electrode (GCE, 3 mm in diameter) as the working electrode (WE), a platinum counter electrode (CE) and a Ag/AgCl (sat. KCl) reference electrode (RE).

2.3. Preparation of NPG

NPG was made by selective dissolution (dealloying) of silver from Ag–Au alloy according to the reported method.[37] Briefly, a piece of commercially available white gold leaf (Ag–Au alloy, 50 : 50, wt%, 100 nm thick) was floated onto 1 : 1 concentrated nitric acid for 10–15 min. The Ag content in the alloy samples could be controlled by selecting the immersion time. Then the NPG foil was washed to neutral with Milli-Q water to remove the NO_3^- and Ag^+, which could interfere with signal detection during ECL analysis. Then the NPG foil was taken out and coated on the surface of the GCE.

2.4. Preparation of CNCs

The electrochemical preparation of CNCs was performed in an electrochemical cell consisting of a graphite rod (GR) working electrode, a Pt mesh counter electrode, a Ag/AgCl reference

electrode, and pH 7.0 phosphate buffer solution (PBS). The applied potential at the GR electrode was cycled between −3.0 and 3.0 V at 0.1 V s^{-1}. As the number of scan cycles increased, the electrolyte solution changed from colorless to yellow and finally to dark brown after 30 cycles. The dark brown solution was centrifuged (13 500*g*) for 10 min to remove the non-fluorescent deposit. The supernatant was further dialyzed against water through a dialysis membrane (MWCO of 1 kDa) to remove inorganic salt. Then the CNCs were obtained by ultrafiltering the solution through centrifugal filter devices with a 3 kDa MWCO membrane.

2.5. Preparation of PdCu bimetallic nanocomposites

The PdCu bimetallic nanocomposites were produced as described previously.[32] In brief, the NPC were fabricated by dealloying CuAl alloys in 1.0 M NaOH for 5 h at 30 °C. The NPC samples were stored in N_2 saturated ultrapure water to avoid oxidation. In a typical replacement reaction, 10 mg of freshly made NPC was quickly added into K_2PdCl_4 aqueous solution (1.2 mM, 150 mL) in a three-neck flask. The reaction was performed at 5 °C under N_2-protected magnetic stirring conditions for 150 min.

2.6. Preparation of PdCu@CNCs composites conjugated DNA (S_3)

Briefly, CNCs were first loaded on PdCu bimetallic nanocomposites based on cysteamine *via* the EDC–NHS coupling. Namely, 1 mL of PdCu alloys (4.67 μM) were incubated with 0.2 mL CNCs and 0.02 μM cysteamine, and the concentration of EDC–NHS was 10 μM. Then the mixture was incubated under oscillating conditions for 1 h. The cysteamine was immobilized on the PdCu alloy surface *via* the –SH bond, and then the $–NH_2$ moiety at cysteamine would react with the –COOH group of CNCs, resulting in covalently bound CNCs at the PdCu alloy surface. The S_3 was activated with acetate buffer (pH 5.2) and 1.5 μL of 10 mM TCEP for 1 h, and then added into the mixture to a final concentration of 0.02 μM. The resulting ECL nanoprobes were separated by centrifugation.

2.7. Fabrication of the DNA sensor based on NPG electrode and PdCu@CNCs composites

The whole process for constructing the modified electrode is shown schematically in Fig. 1. A GCE electrode with 3 mm diameter was polished carefully with 1.0, 0.3 and 0.05 μm alumina powder on fine abrasive paper and washed ultrasonically with water. NPG electrode freshly prepared was immediately used for the preparation of DNA biosensor by immersing the electrode into an immobilization buffer containing 1.0×10^{-8} M capture probe (S_1) for 2 h. The DNA-modified electrode was further treated with 1.0 mM MCH for 2 h to obtain a well-aligned DNA monolayer, followed by washing with water to remove unspecific adsorbed DNA. For the hybridization reaction, ssDNA–NPG was immersed into stirred Tris–HCl solution containing target DNA (S_2) for a desired time at 37 °C. The DNA-modified NPG electrode was secondly hybridized with reporter probes (S_3) loaded with PdCu@CNCs composites for 3 h at room temperature. After hybridization, the electrode was extensively rinsed with washing buffer (10 mM Tris–HCl, pH 7.4) and dried under a stream of nitrogen prior to electrochemical characterization.

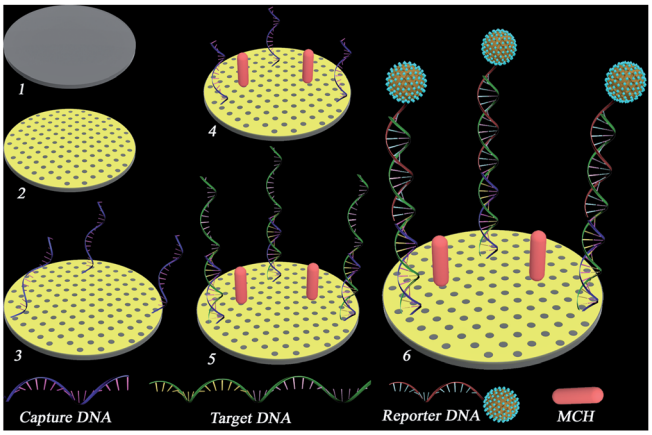

Fig. 1 Schematic representation of the fabrication of the DNA biosensor (1) GCE, (2) GCE assembled with NPG, (3) after immobilization of capture DNA (S_1), (4) after blocking with MCH, (5) hybridization with target DNA (S_2), and (6) hybridization with the PdCu@CNCs labeled reporter DNA (S_3).

2.8. ECL detection

ECL measurements were done at room temperature and the potential swept from −0.8 to −1.8 V with scan rate of 100 mV s^{-1} in a solution of 10 mM Tris–HCl buffer (pH 7.4) containing 0.1 M $K_2S_2O_8$ and 0.1 M KCl as the coreactant with a photomultiplier tube voltage of 800 V. The ECL signals related to the target DNA (S_2) concentrations could be measured.

3. Results and discussion

3.1. Characterization of NPG, NPC and PdCu alloy

Fig. 2A shows the transmission electron microscopy (TEM) images of NPG, which displayed a type of sponge-like morphology after 15 min of dealloying, with a 15–20 nm sized pore structure.

Fig. 2B shows the scanning electron microscope (SEM) image of NPC, it was observed that the ligament and pore sizes were uniformly distributed across the entire sample. The average size of the smooth copper ligament was *ca.* 45 nm. The size of the ligament could also be tuned to some extent by varying the reaction parameters such as time, temperature, and post-annealing conditions. The 3D nanoporous material provided a flexible substrate for further functionalization with other catalytic metals like Pd-based nanostructure. In this work, the PdCu bimetallic nanostructure presented uniform 3D nanotubular mesoporous nanostructure. As can be seen in Fig. 2C, it was interesting to find that the shell surfaces are comprised of many small pores and grains around 3 nm instead of being smooth and seamless, implying the formation of a third order porosity at sub 5 nm scale. In order to gain insight into the structural formation and evolution, X-ray diffraction (XRD) was used to examine the crystal structure of PdCu alloy. As shown in ESI, Fig. S1†, the peaks can be assigned to the

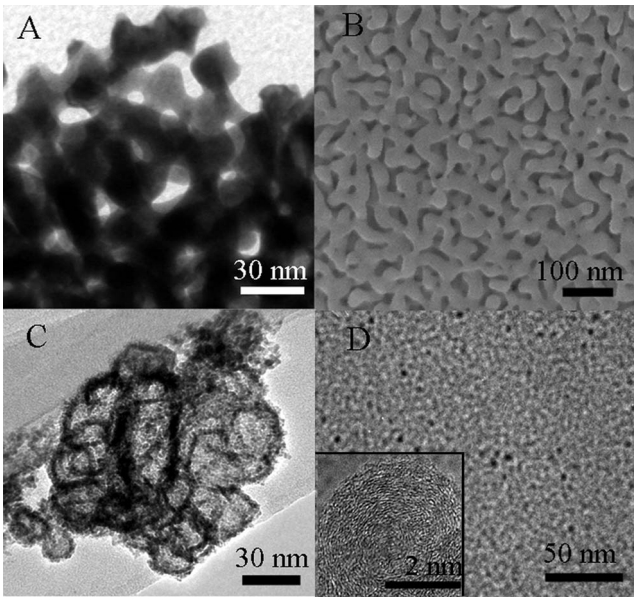

Fig. 2 Representative TEM images of NPG (A), SEM images of NPC (B), TEM of PdCu alloy (C), and TEM of CNCs (D). Inset was the HRTEM images of CNCs.

diffraction of the (111), (200), and (220) planes of face-centered cubic. The well-defined diffraction peaks sit well within the range of the diffractions for PdCu bimetallic nanostructure, indicating the formation of a PdCu alloy structure.

3.2. Characterization of CNCs

As shown in Fig. 2D, characterization of TEM suggests that the size of the CNCs had a uniform spherical shape and was narrowly distributed with diameters in the range of 2–3 nm. The inset is a high-resolution transmission electron microscopy (HRTEM) image of the fluorescent fractions, revealing clearly that CNCs were monodisperse nanocrystals.

The prepared CNCs in solution were further characterized by UV-vis absorption and photoluminescence (PL) spectra (see ESI, Fig. S2†). The UV-vis absorption spectrum revealed the first absorption band at 200 nm. The PL spectra ranged from 440 (blue) to 560 nm (yellow) with increase in the diameter, corresponding to the photoluminescent quantum yield of 27.0%, 18.1% and 12.3%, respectively. The inset shows the bright blue emission from the product chosen in this assay excited by a UV lamp as we monitored the electrolyte solution during the electrochemical process. Additionally, the Fourier transform infrared (FTIR) spectrum for the dried CNC sample showed the CNCs had an abundance of –COOH groups at their surfaces, which benefits CNC labeling.[38]

3.3. Characterization of the NPG-based DNA biosensor

The morphology of GCE and hybridization with the PdCu@CNCs labeled reporter DNA was characterized in ESI, Fig. S3†. As can be seen from the SEM images, the NPG was assembled on the surface of GCE, and the PdCu@CNCs labeled reporter DNA was also hybridized with target DNA, thus assembled on the surface of GCE.

Electrochemical impedance spectroscopy (EIS) was an effective method for probing the features of surface-modified electrodes. The assembly of oligonucleotides on electrodes and the formation of double-stranded DNA could be followed by EIS. Fig. 3 shows the Nyquist plots of impedance for the stepwise modification process with the NPG electrode (Fig. 3A) and bare flat Au electrode (Fig. 3B). For the bare flat Au electrode as shown in Fig. 3B, the impedance spectra included a semicircle portion at higher frequencies compared with NPG electrode in Fig. 3A relating to the electron transfer-limited process and a linear portion at lower frequencies corresponding to diffusion. The increase in the diameter of the semicircle reflected the increase in the interfacial charge-transfer resistance (R_{ct}).

The NPG electrode exhibited an almost straight line, which is characteristic of the diffusional limiting step of the electrochemical process. Even after probe immobilization and hybridization steps, the R_{ct} values were also quite low, indicating that the NPG electrode represented high conductivity due to its 3D nanoporous structure.[39] The results demonstrated that the NPG electrode was fabricated as expected.

3.4. Electrochemical and ECL behaviors of the PdCu@CNCs composite

The ECL electrodes were scanned from −0.8 to −1.8 V in 10 mM Tris-HCl buffer (pH 7.4) containing 0.1 M $K_2S_2O_8$ and 0.1 M KCl. The ECL mechanism of the CNCs was proposed to involve the formation of excited-state CNCs(R) *via* electron-transfer annihilation of positively charged (R^+) and negatively charged CNCs (R^-). The ECL behavior of CNCs in the presence of peroxydisulfate ($S_2O_8^{2-}$) was suggested to involve the electron-transfer annihilation of negatively charged CNCs (R^-) and the strongly oxidizing $SO_4^{\cdot-}$ radicals (generated by electroreduction of $S_2O_8^{2-}$),[38] which might be involved in the CNCs–$S_2O_8^{2-}$ ECL process. The success of the biobarcode amplification was closely related to the abundant loading of the CNCs conjugated with PdCu alloy. Therefore, in order to demonstrate the amplification properties of PdCu@CNCs composite, a control experiment without the involvement of PdCu alloy was carried out. In Fig. 4, curve (a) showed ECL–potential curve of the pure CNCs labeled S_3, and curve (b) showed the ECL–potential curve of the PdCu@CNCs composite labeled S_3. The quantity of the CNCs

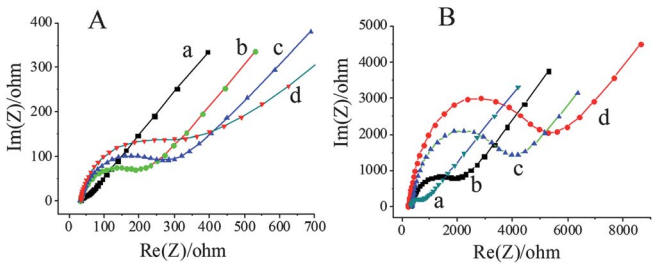

Fig. 3 Nyquist plots corresponding to NPG electrode (A) and flat Au electrode (B). (a) The bare electrode, (b) after immobilization of capture DNA (S_1), (c) hybridization with target DNA (S_2), and (d) hybridization with the PdCu@CNCs labeled reporter DNA (S_3). The data were performed in the presence of Tris-HCl buffer (2.5 mM $Fe(CN)_6^{4-/3-}$+0.1 M KCl, pH 7.4). The frequency range is between 0.01 and 100 000 Hz with signal amplitude of 5 mV.

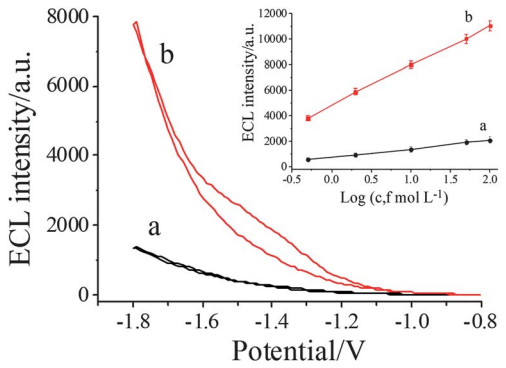

Fig. 4 ECL–potential curves of (a) pure CNCs-labeled S_3, (b) PdCu@CNCs composites labeled S_3 in 10 mM Tris-HCl buffer (pH 7.4) containing 0.1 M $K_2S_2O_8$ and 0.1 M KCl. The S_3 concentration was 1.0×10^{-14} M. Scan rate: 100 mV s^{-1}. The voltage of the PMT was 800 V.

and PdCu@CNCs composites were equal in both labels. As can be seen in Fig. 4, the PdCu@CNCs composite labeled S_3 revealed excellent ECL performance compared with pure CNCs. The ECL intensity of the DNA biosensor using PdCu@CNCs composites labeled S_3 was 6 times higher than the pure CNCs labeled S_3. From the inset, we can see that the NPG-electrode by PdCu@CNCs composites exhibit excellent ECL performance.

One reason for this may be that the cysteamine could urge self-assembly of the CNCs onto PdCu alloy, the sulfur atoms of the cysteamine are applied to bind to the PdCu surface while the amino groups are employed for the attachment of CNCs through EDC–NHS, and the SH-group of S_3 also had a tendency to be adsorbed on the surface of PdCu bimetallic nanostructures.[40,41] Due to the advantage of low cytotoxicity of CNCs, the ECL nanoprobe had good biocompatibility.[21] The nanotubular mesoporous PdCu alloy showed superior activity for important electrode reactions such as oxygen reduction reaction, which indicated that PdCu@CNCs composite had the larger surface area, fascinating electrocatalytic activity and excellent conductivity for facilitating the ECL reaction.[32] Therefore, the PdCu@CNCs composite had highly effective ECL properties, which were promising for the construction of the ECL biosensor.

3.5. Optimization of experimental conditions

The effect of incubation time of PdCu@CNCs composites with thiols on ECL intensity was extensively investigated (see ESI, Fig. S4†). Fig. S4† shows the ECL calibration curves obtained upon different incubation time (1, 2, 3, 4, and 6 h) of PdCu@CNCs composites and S_3. As can be seen from Fig. S4†, ECL intensity of the ECL nanoprobes increased as the incubation time extended. However, when the time came to 3 h, the current signal began to level off, suggesting that the binding sites of PdCu@CNCs composites were replaced by thiols absolutely, so the optimal incubation time was 3 h.

To obtain the maximal ECL intensity, the effects of hybridization temperature on the hybridization reaction was investigated as shown in Fig. S5–S6 in the ESI†. The hybridization temperature was studied in the range from 20 °C to 90 °C. As can be seen in Fig. S5†, the hybridization temperature of S_1 and S_2 reached a maximum ECL intensity at 42 °C, and the optimal incubation temperature of S_2 and PdCu@CNCs labeled S_3 was 42 °C (Fig. S6†).

3.6. Sensitive detection of target DNA

Under the optimal conditions, the ECL intensity for the NPG-based sensor after hybridization with different concentrations of target DNA (S_2) is shown in Fig. 5A. The inset was the calibration curve for the determination of S_2. As can be seen in Fig. 5A, the ECL intensity was found to be logarithmically related to the concentration of S_2 over the range 5.0×10^{-17} to 8.0×10^{-12} M. The regression equation was $I_{ECL} = 5065.3 + 3116.4 \log c_{DNA}$ (c_{DNA} per mol L^{-1}) and the correlation coefficient was 0.9982 ($n = 6$). A detection limit of 18 aM S_2 can be estimated using 3σ, indicative of an acceptable quantitative behavior. The relative standard deviation of eleven replicate determinations of S_2 was 3.8%, 2.5% and 2.7% at 0.1, 5.0 and 50 fM ($n = 11$), respectively. The results demonstrate that the proposed method could be used for the ultrasensitive determination of S_2. The reproducibility of the calibration curve is shown in Fig. 5B. Curve (a), (b) and (c) showed the calibration curve of target DNA, single base mismatched DNA and non-*c*DNA, respectively. The result shows that the target DNA presented the good linear range. Moreover, Table 1 shows the linear range and detection limit of DNA biosensor with previous reports.[2,42–47] The limit of detection was much lower than those of 500 aM–60 nM for the reported competitive biosensors (Table 1). The PdCu@CNCs composite as novel ECL labels with amplification technique greatly increased the sensitivity and extended the detectable concentration range by 3 orders of magnitude. Compared with other methods, the DNA biosensor had a relatively large linear range and low detection limit.

3.7. Specificity, stability, reproducibility, and regeneration of the DNA biosensor

The specificity of the present biosensor in discriminating perfect target DNA from single base mismatched and non*c*DNA sequences was tested *via* comparing the ECL signal changes brought under three concentrations as shown in Fig. 6. Referring to the complementary hybridization at each concentration as 100%, Fig. 6 showed that mismatched DNA (S_4) and non*c*DNA

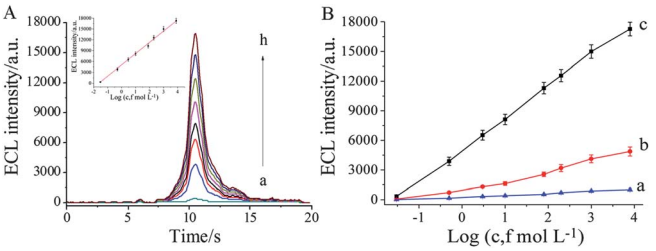

Fig. 5 (A) ECL profiles of the DNA biosensor in the presence (a–g) of different concentrations of S_2 in 10 mM Tris-HCl buffer (pH 7.4) containing 0.1 M $K_2S_2O_8$ and 0.1 M KCl. S_2 concentration (fM): (a) 0.03, (b) 0.5, (c) 3, (d) 10, (e) 80, (f) 200, (g) 1000, (h) 8000 (the voltage of the photomultiplier tube was set at 800 V). Insert is the calibration curve of the DNA biosensor. (B) The reproducibility of the calibration curve. Curve (a), (b) and (c) show the calibration curve of target DNA, single base mismatched DNA and non*c*DNA, respectively.

Table 1 The results of comparing with other reported techniques for the determination of DNA

Analytical techniques	Label or indicator	Linear range	Detection limit of ssDNA	References
Electrical detection	AuNPs with Ag amplification	0.5–50 nM	5 pM	2
EIS	Methylene blue	20–100 nM	0.1 nM	42
Colorimetric	AuNPs	60–500 nM	60 nM	43
Fluorescence	ZnS and CdSe QDs	4–1000 nM	2 nM	44
Chronocoulometry	AuNPs	0.05–10 pM	10 fM	45
Flow injection chemiluminescence	nanoCuS tags	2.0–100 pM	0.55 pM	46
Chemiluminescence	AuNPs and CuS–NPs	0.02–2 pM	4.8 fM	47
Electrochemiluminescence	PdCu–CNCs composites	0.05–8000 fM	18 aM	This work

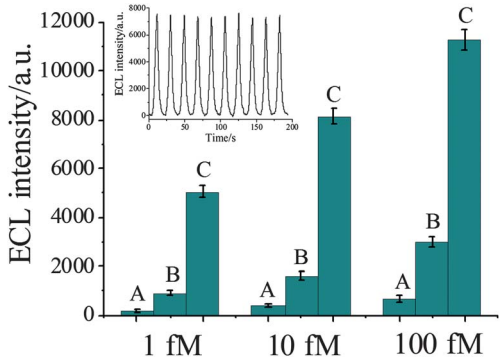

Fig. 6 Comparison of ECL signal with a series of target DNA (1.0×10^{-15}, 1.0×10^{-14}, and 1.0×10^{-13} M): the target DNA (C), one-base mismatched DNA (B), and completely mismatched target DNA (A). Error bars showed the standard deviations of measurements. The inset was the stabilization of ECL emission of 1.0×10^{-13} M target DNA on NPG-electrode in 10 mM Tris-HCl buffer (pH 7.4) containing 0.1 M $K_2S_2O_8$ and 0.1 M KCl, under continuous cyclic scans between −0.8 to −1.8 V for 10 cycles. Scan rate, 100 mV s^{-1}.

(S_5) did not exhibit any great decrease of signal. The ratio of hybridization efficiencies were as follows: target : Ms : Nc (target DNA : single base mismatched DNA : non*c*DNA) = 100 : 18 : 4, 100 : 20 : 5, and 100 : 26 : 6 for 1.0×10^{-15}, 1.0×10^{-14}, and 1.0×10^{-13} M targets, respectively. The results show that only the perfectly matched DNA produced prominent signals. The comparison essentially suggested that our DNA biosensor represented a high specificity and could be satisfactory to single-nucleotide polymorphism assays.

The inset in Fig. 6 is the ECL signal–time curve under continuous potential scanning for 10 cycles. After the DNA biosensor was stored in pH 7.4 Tris-HCl buffer at 4 °C for over 2 months, it was used to detect the same S_2 concentration, the ECL intensity of the NPG-based sensor using PdCu@CNCs composites labeled S_3 decreased to about 92% of its initial response, demonstrating that the DNA biosensor had good potential cycling stability.

The reproducibility of the DNA biosensor was estimated with intra- and inter-assay precision. The intra-assay precision was evaluated by assaying one S_2 level for four replicate measurements. The inter-assay precision was estimated by determining one S_2 level with four immunosensors made at the same electrode. The intra- and inter-assay variation coefficients (CVs) obtained from 1.0×10^{-14} M S_2 were 6.2% and 7.3%, respectively. Obviously, the inter-assay CV showed a good electrode-to-electrode reproducibility of the fabrication protocol, while the low value of intra-assay CV indicated that the immunosensor could be regenerated and used repeatedly.

In our test, the DNA biosensor could be regenerated by incubation of the modified electrode in hot water (90 °C) for 1 min, by which hybridized DNA was removed *via* thermal denaturation. As shown in ESI in Fig. S7†, the as-renewed electrode could restore 89.7%, and 91% of the initial value for unheated modified electrode at S_2 concentrations of 5 fM and 10 fM, respectively. The electrode was evaluated by five replicative measurements, showing accepted reusability. The consecutive measurements were repeated five times and a RSD of 5.2% was acquired. The DNA biosensor could be stored in the refrigerator for one week with negligible loss of the immobilized probe DNA.

3.8. Application of the DNA biosensor in human serum samples

In an attempt to test the applicability of our DNA biosensor for detection in real samples, we employed diluted human serum samples (1 : 10). The control experiments were performed in the human serum without any oligonucleotides. Fig. 7 shows that there is little discernible signal when a single-mismatched (SM) is present compared to the control. Significantly, the ECL signals can be observed corresponding to the presence of target DNA that was comparable to that obtained in pure DNA solutions. The results demonstrate the ability of our DNA biosensor to detect perfect matches (PM) in human serum, which would therefore offer an approach for accurate gene diagnostics.

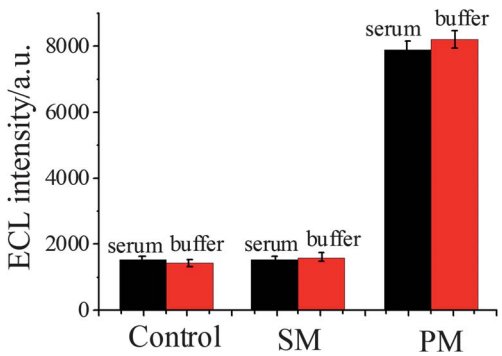

Fig. 7 Histograms for ECL intensities at different conditions. From left to right: a human serum sample, a pure buffer sample, 10 fM single-base mismatches in the human serum, 10 fM single-base mismatches in the pure buffer, 10 fM perfect matches in the human serum, and 10 fM perfect matches in the pure buffer.

4. Conclusions

To conclude, we have successfully developed an ECL biosensor *via* introduction of a novel ECL nanoprobe (PdCu@CNCs composites) based on NPG electrode. As shown by our research, this assay allows us to determine oligonucleotides down to 18 aM with high sensitivity and selectivity. The main advantages of the present biosensor contributed to two aspects. First, the fabrication of NPG electrode with high active surface area can greatly enhance the immobilization of captured DNA. Second, a novel ECL label of PdCu@CNCs composites was obtained with excellent ECL activity. It is demonstrated that the trimodal hollow bimetallic structure in nanotubular mesoporous PdCu bimetallics plays a crucial role for the enhancement of ECL signal. Moreover, this method was stable and provides a promising platform to fabricate cost-effective, simple, robust, and reusable DNA biosensors, which has great potential in point-of-care applications for accurate gene diagnostics.

Acknowledgements

This work was financially supported by the Natural Science Research Foundation of China (21175058, 51003039), Technology Development Plan of Shandong Province, China (Grant no. 2011GGB01153), and State Key Laboratory of Environmental Chemistry and Ecotoxicology Research Center for Eco-Environmental Sciences Chinese Academy of Sciences Open Foundation (KF2011-03).

References

1 T. G. Drummond, M. G. Hill and K. B. Jacqueline, *Nat. Biotechnol.*, 2003, **21**, 1192.
2 S. J. Park, T. A. Taton and C. A. Mirkin, *Science*, 2002, **295**, 1503.
3 E. G. Hvastkovs and D. A. Buttry, *Anal. Chem.*, 2007, **79**, 6922.
4 W. Y. Chen, G. Y. Lan and H. T. Chang, *Anal. Chem.*, 2011, **83**, 9450.
5 L. G. Xu, Y. Y. Zhu, W. Ma, H. Kuang, L. Q. Liu, L. B. Wang and C. L. Xu, *J. Phys. Chem. C*, 2011, **115**, 16315.
6 W. M. Zheng and L. He, *J. Am. Chem. Soc.*, 2009, **131**, 3432.
7 J. Xu, K. W. Liu, K. S. Matthews and S. L. Biswal, *Langmuir*, 2011, **27**, 4900.
8 Y. Hoshino, T. Kawasaki and Y. Okahata, *Biomacromolecules*, 2006, **7**, 682.
9 J. Zhang, R. J. Lao, S. P. Song, Z. Y. Yan and C. H. Fan, *Anal. Chem.*, 2008, **80**, 9029.
10 A. K. Boal and J. K. Barton, *Bioconjugate Chem.*, 2005, **16**, 312.
11 L. Z. Hu, Z. Bian, H. J. Li, S. Han, Y. L. Yuan, L. X. Gao and G. B. Xu, *Anal. Chem.*, 2009, **81**, 9807.
12 T. Endo, K. Kerman, N. Nagatani, Y. Takamura and E. Tamiya, *Anal. Chem.*, 2005, **77**, 6976.
13 R. Wilson, C. Clavering and A. Hutchinson, *Anal. Chem.*, 2003, **75**, 4244.
14 W. J. Miao, *Chem. Rev.*, 2008, **108**, 2506.
15 A. J. Bard, Z. F. Ding and N. Myung, *Struct. Bonding*, 2005, **118**, 1.
16 F. Erogbogbo, C. A. Tien, C. W. Chang, K. T. Yong, W. C. Law, H. Ding, I. Roy, M. T. Swihart and P. N. Prasad, *Bioconjugate Chem.*, 2011, **22**, 1081.
17 X. Michalet, F. F. Pinaud, L. A. Bentolila, J. M. Tsay, S. Doose, J. J. Li, G. Sundaresan, A. M. Wu, S. S. Gambhir and S. Weiss, *Science*, 2005, **307**, 538.
18 A. M. Derfus, W. C. W. Chan and S. N. Bhatia, *Nano Lett.*, 2004, **4**, 11.
19 S. N. Baker and G. A. Baker, *Angew. Chem., Int. Ed.*, 2010, **49**, 6726.
20 L. Cao, X. Wang, M. J. Meziani, F. S. Lu, H. F. Wang, P. G. Luo, Y. Lin, B. A. Harruff, L. M. Veca, D. Murray, S. Y. Xie and Y. P. Sun, *J. Am. Chem. Soc.*, 2007, **129**, 11318.
21 Q. L. Zhao, Z. L. Zhang, B. H. Huang, J. Peng, M. Zhang and D. W. Pang, *Chem. Commun.*, 2008, 5116.
22 Z. A. Qiao, Y. F. Wang, Y. Gao, H. W. Li, T. Y. Dai, Y. L. Liu and Q. S. Huo, *Chem. Commun.*, 2010, **46**, 8812.
23 K. Welsher, Z. Liu, D. Daranciang and H. J. Dai, *Nano Lett.*, 2008, **8**, 586.
24 M. J. O'Connell, S. M. Bachilo, C. B. Huffman, V. C. Moore, M. S. Strano, E. H. Haroz, K. L. Rialon, P. J. Boul, W. H. Noon, C. Kittrell, J. Ma, R. H. Hauge, R. B. Weisman and R. E. Smalley, *Science*, 2002, **297**, 593.
25 Y. Sun, S. R. Wilson and D. I. Schuster, *J. Am. Chem. Soc.*, 2001, **123**, 5348.
26 A. M. Lebedev, K. A. Menshikov, V. G. Stankevich, N. Y. Svechnikov, A. V. Ryzkova, O. V. Boltalina, I. V. Goldt, I. N. Ioffe, I. A. Kamenskikh and L. N. Sidorov, *Nucl. Instrum. Methods Phys. Res.*, 2005, **543**, 221.
27 J. G. Zhou, C. Booker, R. Li, X. T. Zhou, T. K. Sham, X. L. Sun and Z. Ding, *J. Am. Chem. Soc.*, 2007, **129**, 744.
28 J. L. Gole and E. Veje, *J. Phys. Chem. B*, 2006, **110**, 2064.
29 J. Lu, J. X. Yang, J. Z. Wang, A. L. Lim, S. Wang and K. Ping, *ACS Nano*, 2009, **3**, 2367.
30 A. Petushkov, J. Intra, J. B. Graham, S. C. Larsen and A. K. Salem, *Chem. Res. Toxicol.*, 2009, **22**, 1359.
31 J. Erlebacher, M. J. Aziz, A. Karma, N. Dimitrov and K. Sieradzki, *Nature*, 2001, **410**, 450.
32 C. X. Xu, Y. Zhang, L. Q. Wang, L. Q. Xu, X. F. Bian, H. Y. Ma and Y. Ding, *Chem. Mater.*, 2009, **21**, 3110.
33 C. X. Xu, J. X. Su, X. H. Xu, P. P. Liu, H. J. Zhao, F. Tian and Y. Ding, *J. Am. Chem. Soc.*, 2007, **129**, 42.
34 C. X. Xu, X. H. Xu, J. X. Su and Y. Ding, *J. Catal.*, 2007, **252**, 243.
35 A. W. Zhu, Y. Tian, H. Q. Liu and Y. P. Luo, *Biomaterials*, 2009, **30**, 3183.
36 B. C. Tappan, S. A. Steiner and E. P. Luther, *Angew. Chem., Int. Ed.*, 2010, **49**, 4544.
37 M. N. Kashid and L. K. Minsker, *Ind. Eng. Chem. Res.*, 2009, **48**, 6465.
38 L. Y. Zheng, Y. W. Chi, Y. Q. Dong, J. P. Lin and B. B. Wang, *J. Am. Chem. Soc.*, 2009, **131**, 4564.
39 X. J. Chen, Y. Y. Wang, J. J. Zhou, W. Yan, X. H. Li and J. J. Zhu, *Anal. Chem.*, 2008, **80**, 2133.
40 Y. J. Ji, S. Jain and R. J. Davis, *J. Phys. Chem. B*, 2005, **109**, 17232.
41 K. Shimizu, S. Koizumi, T. Hatamachi, H. Yoshida, S. Komai, T. Kodama and Y. Kitayama, *J. Catal.*, 2004, **228**, 141.
42 D. D. Zhang, Y. Peng, H. L. Qi, Q. Gao and C. X. Zhang, *Biosens. Bioelectron.*, 2010, **25**, 1088.
43 K. Sato, K. Hosokawa and M. Maeda, *J. Am.Chem. Soc.*, 2003, **125**, 8102.
44 D. Gerion, F. Q. Chen, B. Kannan, A. H. Fu, W. J. Parak, D. J. Chen, A. Majumdar and A. P. Alivisatos, *Anal. Chem.*, 2003, **75**, 4766.
45 J. Zhang, S. P. Song, L. Y. Zhang, L. H. Wang, H. P. Wu, D. Pan and C. H. Fan, *J. Am. Chem. Soc.*, 2006, **128**, 8575.
46 C. F. Ding, H. Zhong and S. S. Zhang, *Biosens. Bioelectron.*, 2008, **23**, 1314.
47 S. S. Zhang, H. Zhong and C. F. Ding, *Anal. Chem.*, 2008, **80**, 7206.

